

Edge excitations of bosonic fractional quantum Hall phases in optical lattices

Jonas A. Kjäll¹ and Joel E. Moore^{1,2}

¹*Department of Physics, University of California, Berkeley, CA 94720*

²*Materials Sciences Division, Lawrence Berkeley National Laboratory, Berkeley, CA 94720*

(Dated: November 18, 2018)

The rapid development of artificial gauge fields in ultracold gases suggests that atomic realization of fractional quantum Hall physics will become experimentally practical in the near future. While it is known that bosons on lattices can support quantum Hall states, the universal edge excitations that provide the most likely experimental probe of the topological order have not been obtained. We find that the edge excitations of an interacting boson lattice model are surprisingly sensitive to interedge hybridization and edge-bulk mixing for some confining potentials. With properly chosen potentials and fluxes, the edge spectrum is surprisingly clear even for small systems with strong lattice effects such as bandwidth. Various fractional quantum Hall phases for bosons can be obtained, and the phases $\nu = 1/2$ and $\nu = 2/3$ have the edge spectra predicted by the chiral Luttinger liquid theory.

Fractional quantum Hall (FQH) phases contain a wide variety of interesting physics, including topologically degenerate ground states, fractional bulk excitations, and gapless chiral edge excitations. They arise at low temperatures when strong magnetic fields are applied to high-quality two-dimensional electron gases with low carrier concentration. Ultracold gases of neutral atoms are being used to investigate several properties of materials which can be hard to control precisely in the solid state. As these systems are charge-neutral, an ordinary magnetic field cannot be used to create the Lorentz force. A synthetic magnetic field can be created by rotation, but technical issues appear to limit this approach to lower field strengths than are necessary for FQH [1], with the exception of a recent experiment with few trapped particles [2].

Recently, several theoretical [3–5] and experimental [1, 6] proposals have been made for stronger synthetic magnetic fields for ultracold neutral atoms. All of them can be used with optical lattices which enhance interaction effects and give a larger energy gap above the FQH ground state. Theoretical work on lattice systems with an effective magnetic field goes back at least to Hofstadter’s work [7] on non-interacting particles; the FQH phases are strongly interacting, and Sørensen et al. [3] showed that in the low flux limit and strong interactions the system could be well described by Laughlin’s wavefunction. In subsequent work Hafezi et al. [8] showed that this could be extended to larger fluxes per unit cell by investigating the topological structure of the ground state.

The goal of this work is to understand practical experimental conditions for observation of edge states in bosonic lattice FQH systems and compare numerical results for edge excitations in hierarchy states to the prediction of chiral Luttinger liquid theory [9]. Convincing observation of bosonic fractional quantum Hall states will depend on an experimentally viable probe of the topological order; while many multi-particle quantities have been used to diagnose the topological state in past theoretical work, such as ground state degeneracy, bulk energy gap,

wavefunction overlap, band flatness, band Chern number and entanglement spectra, these are not yet experimentally accessible. Our focus will be on edge excitations, whose “universal” aspects contain information about the topological order of the system, although a good understanding of the “non-universal” effects of the lattice and trap is crucial for these excitations to provide a clear signal that an FQH phase has been obtained.

While this paper focuses on bosonic hierarchy states, bosonic systems can also realize some specific FQH lattice states without analog in the continuum [10]. We consider lattices with uniform flux; recent work has shown convincingly that non-uniform magnetic fields can create the same FQH phases without Landau levels [11–15]. The lessons in this work for trapping potentials and geometries apply also to these more complex situations.

We investigate bosonic FQH phases in the simplest lattice system, hard-core bosons on a square lattice in a uniform magnetic field with equivalent Landau level filling $\nu = N/N_\phi$. N is the number of bosons in the system and N_ϕ is the number of fluxes, measured in units of the magnetic flux quantum $\Phi_0 = hc/q$, for particles of charge q . The modified Bose-Hubbard Hamiltonian is,

$$H = -J \sum_{\vec{r}} \hat{a}_{\vec{r}+\hat{x}}^\dagger \hat{a}_{\vec{r}} e^{-i\alpha_x y} + \hat{a}_{\vec{r}+\hat{y}}^\dagger \hat{a}_{\vec{r}} e^{i\alpha_y x} + h.c., \quad (1)$$

where $\hat{a}_{\vec{r}}^\dagger$ creates a boson on site $\vec{r} = (x, y)$. We use two different gauges for the phases $\vec{\alpha} = (\alpha_x, \alpha_y)$, Landau gauge $\vec{\alpha} = (\alpha, 0)$ on the cylinder to keep explicit translational symmetry around the circumference, and symmetric gauge, $\vec{\alpha} = (\alpha/2, \alpha/2)$ on the square to keep explicit \mathbb{Z}_4 rotational symmetry. The flux through a plaquette $n_\phi = \alpha/2\pi$ is defined modulo 1 and can be expressed as an artificial magnetic field $\vec{B}^* = n_\phi \Phi_0 / a^2 \hat{n}$, where a is the lattice spacing and \hat{n} the vector normal to the lattice plane. At low flux $n_\phi \ll 1$ is the system effectively in the flat band limit [10], where a continuum description can be used. We focus on larger fluxes where the lattice is important. The magnetic length l_B is of the same order

E	One edge	Two edges				
	$p = EL_e/2\pi\hbar v$	$p = 0$	$p = 1$	$p = 2$	$p = 3$	$p = 4$
0	GS	GS				
$2\pi\hbar v/L_e$	1		1R			
$4\pi\hbar v/L_e$	2	1R1L		2R		
	11			1R1R		
$6\pi\hbar v/L_e$	3		2R1L		3R	
	21		1R1R1L		2R1R	
	111			1R1R1R		
$8\pi\hbar v/L_e$	4	2R2L		3R1L		4R
	31	2R1L1L		2R1R1L		3R1R
	22	1R1R2L		1R1R1R1L		2R2R
	211	1R1R1L1L				2R1R1R
	1111					1R1R1R1R

TABLE I. Labeling of the edge spectra for one edge and two edges. 2 has $l_2 = 1$, 111 has $l_1 = 3$ and so on. All edge levels with energy $E \leq 8\pi v/L_e$ and positive momentum $p \geq 0$ are shown. For two edges, the levels with $p < 0$ are equivalent to those with $p > 0$, except L is exchanged for R and vice versa.

as the lattice spacing for the fluxes we are interested in, $l_B = \sqrt{\hbar c/(qB^*)} = a/\sqrt{2\pi n_\phi} \sim a$.

The optical trapping potential $V_{\text{trap}}(x, y)$, provides the equivalent of the electric field confinement in semiconductors. In this paper, we only present results for harmonic traps $V_{\text{trap}}(x, y) = c_x x^2/(L_x/2 - 1/2)^2 + c_y y^2/(L_y/2 - 1/2)^2$ with $c_x, c_y \geq 0$, that ends with open or periodic boundary conditions. The velocity of a non-interacting particle near the edge is $v = |\nabla V_{\text{trap}}(r_c)|/(n_\phi \hbar c/a^2)$, where r_c is the radius of the ground state droplet. The hydrodynamical approach describes well the chiral Luttinger liquid theory of a Laughlin FQH phase $\nu = 1/m$, with $m = 2, 4, 6, \dots$ for bosons [9]. Defining $\rho(\theta)$ as the one-dimensional density along the edge, the Hamiltonian of the edge waves is

$$H_{1/m} = 2\pi \frac{v}{\nu} \sum_{k>0} \rho_{-k} \rho_k, \quad (2)$$

with $[\rho_k, \rho_{k'}] = \frac{\nu}{2\pi} k \delta_{k+k'}$ where $\rho_k = L_e^{-1/2} \int d\theta e^{ik\theta} \rho(\theta)$, $k = p2\pi\hbar/L_e$ with $p \in \mathbb{N}$ and L_e is the length of the edge. This is the $U(1)$ Kac-Moody algebra, describing a set of k uncoupled harmonic oscillators with energy $\sum_p l_p v \hbar k$ and momentum $\sum_p l_p \hbar k$, where $l_p \in \mathbb{N}$ counts the number of excitations in each. For a single edge, the degeneracy of the edge spectrum is 1, 1, 2, 3, 5, 7, 11, 15, 22, ..., see Tab. I for a labeling of the different states. On a cylinder, there are two edges with momentum in different directions, right moving (R) and left moving (L). The degeneracy of this edge spectrum is 1, 2, 5, 10, 20, ... or (1), (1, 1), (2, 1, 2), (3, 2, 2, 3), (5, 3, 4, 3, 5), ... if momentum resolved (Tab. I).

The spectrum of the Hamiltonian (1) is computed by exact diagonalization. Parts of the model we analyze is shown schematically in Fig. 1(a). The edge excitations in an infinite system are gapless, but become gapped in a finite system. To clearly see them, it is desirable to have a large bulk gap. The bulk gaps on a cylinder at

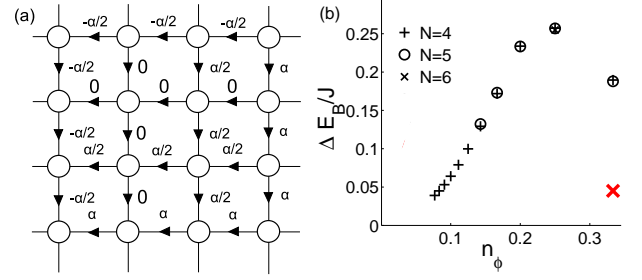


FIG. 1. (Color online) (a) Part of the square lattice in the symmetric gauge with the phases gained when hopping in the direction of the arrows. When hopping in the opposite direction, the phase is the complex conjugate of that shown. (b) The gap $\Delta E_B/J \equiv (E - E_{GS})/J$, for the $\nu = 1/2$ phase on a cylinder, to the lowest bulk excitation as a function of flux per plaquette, for $N = 4 - 6$ particles. The large red symbol corresponds to a spectrum that does not appear to be in a FQH phase.

$\nu = 1/2$ are shown in Fig. 1(b), from calculations in flat infinite wells where edge modes do not exist. The ground state is non-degenerate and the gaps to all excited states are comparable to those reported for a torus [3]. The spectra for $N = 6$ at $n_\phi = 1/3$ is clearly different from the other spectra, indicating that it might not be in a FQH phase. This is in agreement with the lack of a two fold-degeneracy and vanishing wavefunction overlap on a torus for $n_\phi \gtrsim 0.3$ [3]. To get edge excitations in the spectra, more sites outside the ground-state droplet need to be added where the edge waves can propagate. A trapping potential is then essential to confine the condensate. Neglecting the trap for the moment, the wavefunctions in the microscopic theory of edge states for the Laughlin phases are

$$\Psi_{1/m}(z_i) = P(z_i) \prod_{i < j} (z_i - z_j)^m e^{-\sum_i |z_i|^2/4l_B^2}, \quad (3)$$

where $P(z_i) = \sum_p (\sum_i z_i^p)^{l_p}$. This is the form of all zero energy wavefunctions without a trap. For a small number of particles, the edge excitations consisting of few single particle modes $n_p = \sum_p l_p$ extends a distance $\Delta r \lesssim n_p l_B$ outside the ground state droplet.

First, we consider the circular harmonic trap on a square lattice. With an appropriate construction of the \mathbb{Z}_4 symmetric Hamiltonian, a Fourier transform will turn the Hamiltonian into block diagonal form with each block corresponding to a certain angular momentum $L = 0, 1, 2, 3, \dots \text{mod } 4$. These momenta $k_c = \hbar \Delta L/r_c$, are the same as in the Kac-Moody algebra $k = 2\pi \hbar p/(2\pi r_c)$. The analytic edge spectrum for the $\nu = 1/2$ phase is shown in Fig. 2(a). In a system with finite number of particles N , we only expect excitations consisting of $n_p \leq N$

single modes. The energy is proportional to the angular momentum for the trapped phase, indicated by the straight dotted lines. With only $N = 4$ particles on a 11×11 site lattice in a trap $c_a/J = 0.5$, we get remarkably good edge spectras. At $n_\phi = 1/5$, the degeneracies $1, 1, 2, 3, 5, 6, 9, 11, 15, \dots$ in the edge spectra, agreeing with $n_p \leq N$ for $\nu = 1/2$, is clearly visible, see Fig. 2(b). The small energy splitting is due to finite size effects, most noticeable in the states that extends furthest in the trap. Note that all of these state appear to be edge states; there are no bulk excitations for $\Delta E/J \lesssim 0.35$, much larger than the anticipated gap $\Delta E_B/J \approx 0.23$. To experimentally measure the edge spectra, the difference in angular momentum ΔL as the system is excited by an energy E should be measured, leading to the linear relation, the edge velocity $v = E/(\hbar\Delta L/r_c)$. Inserting typical experimental values $J = \hbar/\tau_{\text{tunnel}}$, with the tunneling time $\tau_{\text{tunnel}} = 0.2$ ms and $a = 400$ nm for this setup gives $v \approx 0.2$ mm/s.

There are several states [Fig. 2(b)] that do not belong to the $\nu = 1/2$ edge spectra. The lowest of those states has a $\nu = 2/3$ filling factor. The $\nu = 2/3$ FQH phase has a 3-fold degeneracy on a torus and Möller et al. [16] showed it has a good average overlap with the composite-fermion wavefunction for $n_\phi \lesssim 0.3$ on a lattice. By varying the magnetic flux, it is clear what states belongs to which phase, see Fig. 2(c) for some examples, where the energy difference $\Delta E/J \equiv (E^\nu - E_{GS}^{1/2})/J$ as a function of flux is shown. At small flux per plaquette, our system can become too small for some of the excited states of $\nu = 1/2$. Also, more states move down to the low energy spectra as the flux is decreased. The first is a phase with filling factor $\nu = 3/2$. Upon decreasing the flux further, other phases appear with a ground state filling factor that agrees with some of the phases in the Read-Rezayi sequence for bosons $\nu = g/2$, where $g \in \mathbb{N}$ [17]. Whether these phases actually are FQH phases are left for future studies. Again, around $n_\phi \approx 0.3$, the edge spectra break down and it is unclear what phases exist for $n_\phi \gtrsim 0.3$.

The $\nu = 2/3$ state consists of two condensates with co-moving edge modes. The two $U(1)$ edge branches propagating in the same direction can have a substantial energy difference as they can be located at different radial locations. This spectrum will have the same degeneracies as two edges on a cylinder $1, (1, 1), (2, 1, 2), (3, 2, 2, 3), \dots$, with the difference that states within $()$ have the same angular momentum, not energy. The edge spectra in Fig. 2(d) is at $n_\phi = 1/8$, where the ground state energy for $\nu = 2/3$ is slightly lower than for $\nu = 1/2$. The $\nu = 1/2$ edge excitations are spaced further apart, but the states $1, 1, 2, 3, 5$ can still be clearly distinguished. The two branches of $\nu = 2/3$ have very different energies, but $1, 2, 5$ can easily be seen under the dotted line corresponding to the lowest energy for the higher momentum states. Some additional low-lying states possibly corresponding to ground state filling factor $\nu = 3/2$ can be

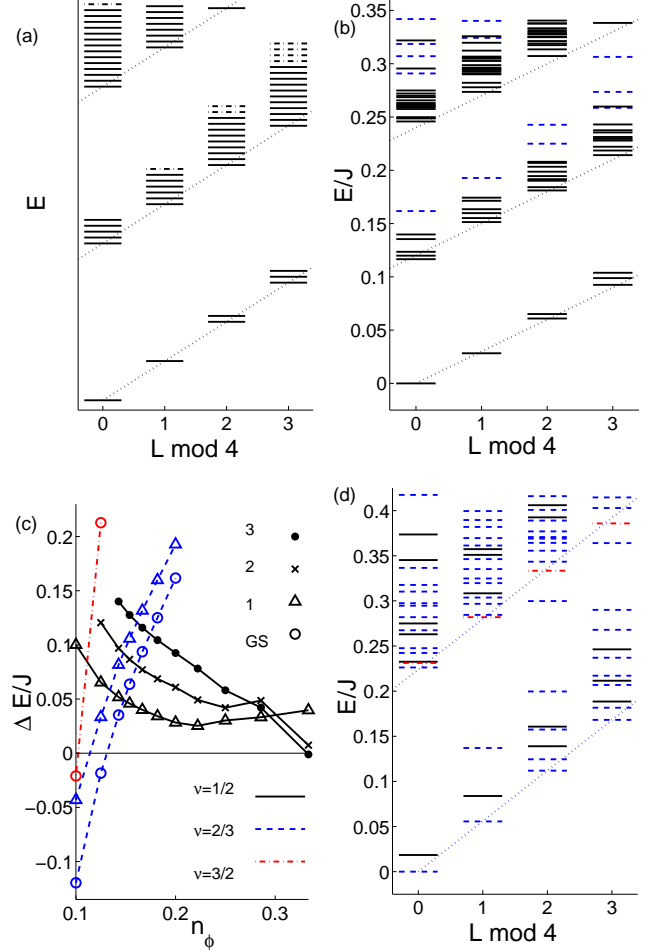


FIG. 2. (Color online) (a) Analytic edge spectra at $\nu = 1/2$ in a trap as a function of angular momenta. Degenerate lines are drawn slightly apart for clarity. The solid lines corresponds to excitations consisting of four single particle modes or less. The dashed dotted lines are the additional excitations appearing for additional modes. (b)-(d) Edge excitations for $N = 4$ particles on a 11×11 square lattice in a circular harmonic trap, $\nu = 1/2$ black solid lines, $\nu = 2/3$ blue dashed lines and $\nu = 3/2$ red dashed dotted lines. (b) Edge spectra at $n_\phi = 1/5$ as a function of angular momentum. (c) Energy gap to the $\nu = 1/2$ ground state for: ground states (\circ), 1 states (\triangle), 2 states (\times) and 3 states (\bullet) as a function of flux per plaquette. (d) Edge spectra at $n_\phi = 1/8$ as a function of angular momentum.

distinguished.

Next, we consider a square lattice on a finite cylinder, which should be a good approximation to an elliptical elongated trap. The cylindrical system in Landau gauge has a \mathbb{Z}_{L_x} symmetry along the circumference of the cylinder, when $\alpha_x = 2\pi/L_x$. With an appropriate construction of the Hamiltonian, a Fourier transform will turn the Hamiltonian into block diagonal form with each block corresponding to a certain momentum $k_x = p_x 2\pi\hbar/L_x = \dots, -2\pi\hbar/L_x, 0, 2\pi\hbar/L_x, \dots \bmod 2\pi\hbar$

along the circumference of the cylinder. These are the same momenta as in the Kac-Moody algebra $k_x = k$.

The edge spectrum as a function of momentum for $N = 4$ particles on a 9×15 site cylinder in a harmonic trap $c_y/J = 0.2$, is shown in Fig. 3(a). Three additional rows are required outside the ground state droplet on both edges to get all edge excitations with $|p_x| \leq N$. No edge excitations with $|p_x| > N$ can be found on these cylinders. The edge states $1R1R1R1L$, $1R1L1L1L$, $1R1R1R1R$ and $1L1L1L1L$ are higher up in the spectra and not shown. The discrepancy from the analytical spectrum, shown in Fig. 3(b), can be explained by two types of finite size effects. The lower-than-expected energy of the high momentum single particle modes depends on their overlap with the opposite edge, and the increase is due to the same reason discussed above for the circular harmonic trap. Bulk excitations are shown with red lines. The bulk gap $\Delta E_B/J \approx 0.12$ is again larger than anticipated, $\Delta E_B/J \approx 0.08$ in Fig. 1(b). The other lines are believed to be edge excitations of other FQH states. The blue dashed lines are states with higher momenta, aliased to a lower momentum $(k_x + \pi \bmod 2\pi) - \pi$. For example, the lowest of those states with $k_x = 2\pi/L_x$ is the ground state translated by 2 lattice sites with momentum $k_x = -2\pi\hbar/9$.

Replacing the harmonic trap with another trap shape does not change the edge spectra qualitatively on a cylinder. However, on a square in a circular trap $V_{\text{trap}} = c_r r^d$ the spectra change completely: the system shows an FQH edge for $1.5 \lesssim d \lesssim 2.5$ with the best spectra at $d = 2$. The other phases in the bosonic Laughlin sequence $\nu = 1/4, 1/6, \dots$ cannot be the ground state without longer range interactions [8], as with hard-core interactions and without a trap, they have the same ground state energy as the $\nu = 1/2$ phase. In a trap, they have energies comparable to higher $\nu = 1/2$ excitations than considered here.

As the magnetic field was decreased, none of the higher order hierarchical states $\nu = 3/4, 4/5, \dots$ was found, but they should appear for larger systems with more particles. The non-abelian phases in the Read-Rezayi sequence $\nu = 1, 3/2, 2, 5/2, \dots$ [17] are believed to be the ground state for bosons in a trap under certain conditions [18], and the $\nu = 3/2$ phase is the simplest bosonic FQH phase that could be used for quantum computing. In the other limit, at large flux per plaquette $n_\phi = p/q + \epsilon$, where p and q are small integers, are the lattice specific FQH phases, believed to appear. For completeness we mention some recent proposals for detecting FQH states in ultracold gases other than by edge properties: imaging the spin-density correlations can allow for the identification of different FQH phases, and the statistics of excited quasiholes can be obtained from the density reduction [19]. The Chern number equals the number of oscillations in the momentum distribution, detectable in time of flight images [20].

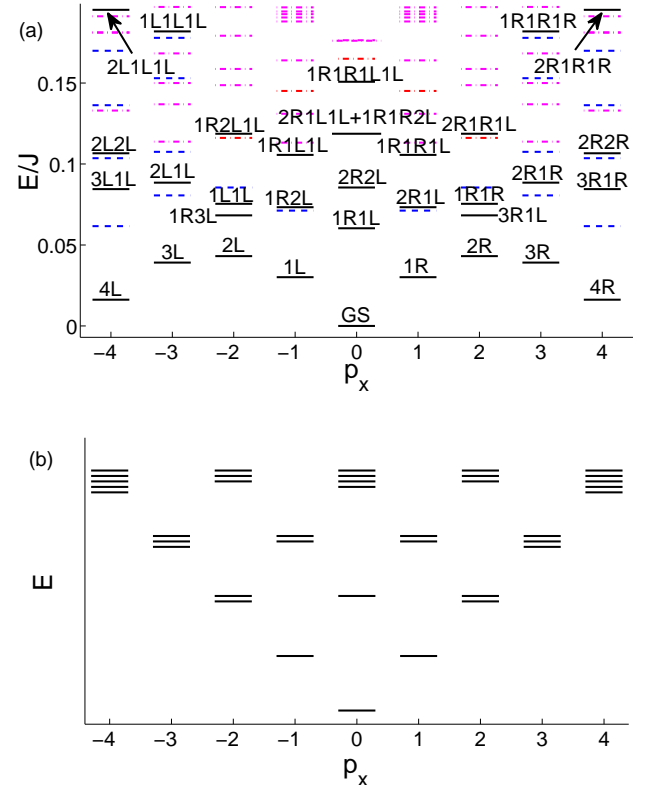


FIG. 3. (Color online) (a) Edge spectra for $N = 4$ particles at $\nu = 1/2$ on a 9×15 site cylinder in a harmonic trap as a function of momenta. Apart from the expected edge spectra (black solid lines), bulk excitations (red dash-dotted lines) and edge excitations from translated $\nu = 1/2$ phases (blue dashed and magenta dashed-dotted lines, where the former are aliased to a lower momenta) are mixed in. Two-fold degenerate states are marked with longer lines. (b) Analytic edge spectra at $\nu = 1/2$ for a large system. Degenerate lines are drawn slightly apart for clarity.

The main result of this work is that hard-core repulsion in a small simple lattice system of approximately square or circular geometry is sufficient to generate clearly resolved edge excitations for the bosonic FQH states at filling $\nu = 1/2$ and $\nu = 2/3$, provided that the conditions described above on flux per site and harmonic trap strength can be achieved; engineering flat or nearly flat bands is unnecessary. In the cylindrical case, the edges are strongly interacting with each other and the edge excitations are much harder to distinguish, which suggests counterintuitively that increasing system size by going to an elongated trap may not be necessary or even desirable. Observation of the bosonic FQH states discussed here would be a logical first step toward even more exciting new states that can be studied by similar methods. The authors acknowledge helpful conversations with R. S. K. Mong and S. Parameswaran and support from the ARO Optical Lattice Emulator program.

-
- [1] Y.-J. Lin, R. L. Compton, K. Jiménez-García, J. V. Porto, and I. B. Spielman, *Nature* **462**, 628 (2009).
- [2] N. Gemelke, E. Sarajlic, and S. Chu, “Rotating few-body atomic systems in the fractional quantum hall regime,” arXiv:1007.2677v1.
- [3] A. S. Sørensen, E. Demler, and M. Lukin, *Phys. Rev. Lett.* **94**, 086803 (2005).
- [4] J. Dalibard, F. G. G. Juzeliunas, and P. Öhberg, *Rev. Mod. Phys.* **83**, 1523 (2011).
- [5] N. R. Cooper, *Phys. Rev. Lett.* **106**, 175301 (2011).
- [6] M. Aidelsburger, M. Atala, S. Nascimbène, S. Trotzky, Y.-A. Chen, and I. Bloch, “Experimental realization of strong effective magnetic fields in an optical lattice,” arXiv:1110.5314v1.
- [7] D. R. Hofstadter, *Phys. Rev. B* **14**, 2239 (1976).
- [8] M. Hafezi, A. S. Sørensen, E. Demler, and M. Lukin, *Phys. Rev. A* **76**, 023613 (2007).
- [9] X.-G. Wen, *Quantum field theory of many body systems* (Oxford University Press, Oxford, 2004).
- [10] L. Hormozi, G. Möller, and S. H. Simon, “Fractional quantum hall effect of lattice bosons near commensurate flux,” arXiv:1109.3434v1.
- [11] E. Tang, J.-W. Mei, and X.-G. Wen, *Phys. Rev. Lett.* **106**, 236802 (2011).
- [12] T. Neupert, L. Santos, C. Chamon, and C. Mudry, *Phys. Rev. Lett.* **106**, 236804 (2011).
- [13] K. Sun, Z. Gu, H. Katsura, and S. Das Sarma, *Phys. Rev. Lett.* **106**, 236803 (2011).
- [14] D. N. Sheng, Z.-C. Gu, K. Sun, and L. Sheng, *Nature Communications* **2**, 389 (2011).
- [15] N. Regnault and B. A. Bernevig, *Phys. Rev. X* **1**, 021014 (2011).
- [16] G. Möller and N. R. Cooper, *Phys. Rev. Lett.* **103**, 105303 (2009).
- [17] N. Read and E. Rezayi, *Phys. Rev. B* **59**, 8084 (1999).
- [18] R. N. Palmer and D. Jaksch, *Phys. Rev. Lett.* **96**, 180407 (2006).
- [19] J. S. Douglas and K. Burnett, *Phys. Rev. A* **84**, 053608 (2011).
- [20] E. Zhao, N. Bray-Ali, C. J. Williams, I. B. Spielman, and I. I. Satija, “Chern numbers hiding in time-of-flight images,” arXiv:1105.3100v2.